Katanin regulates dynamics of microtubules and biogenesis of motile cilia

Neeraj Sharma,[1] Jessica Bryant,[1] Dorota Wloga,[1] Rachel Donaldson,[1] Richard C. Davis,[1] Maria Jerka-Dziadosz,[2] and Jacek Gaertig[1]

[1]Department of Cellular Biology, University of Georgia, Athens, GA 30602
[2]Department of Cell Biology, M. Nencki Institute of Experimental Biology, Polish Academy of Science, 02-093 Warsaw, Poland

The in vivo significance of microtubule severing and the mechanisms governing its spatial regulation are not well understood. In *Tetrahymena*, a cell type with elaborate microtubule arrays, we engineered null mutations in subunits of the microtubule-severing complex, katanin. We show that katanin activity is essential. The net effect of katanin on the polymer mass depends on the microtubule type and location. Although katanin reduces the polymer mass and destabilizes the internal network of microtubules, its activity increases the mass of ciliary microtubules. We also show that katanin reduces the levels of several types of post-translational modifications on tubulin of internal and cortical microtubules. Furthermore, katanin deficiencies phenocopy a mutation of β-tubulin that prevents deposition of polymodifications (glutamylation and glycylation) on microtubules. We propose that katanin preferentially severs older, post-translationally modified segments of microtubules.

Introduction

Microtubules are ubiquitous cytoskeletal polymers made of α/β-tubulin heterodimers that are required for cell motility, intracellular transport, and mitosis/meiosis. Little is known about how organelle-specific properties of microtubules are generated. The length of microtubules is an important parameter that determines the size of cytoskeletal organelles, and affects the distribution of forces generated by microtubule-dependent motors. The length of microtubules can be regulated either by addition/loss of tubulin subunits at the polymer ends, or by internal breakage.

Katanin, a dimer of p60 and p80 proteins (McNally and Vale, 1993), has a strong microtubule-severing activity. p60 is a catalytic subunit that oligomerizes and breaks microtubules while hydrolyzing ATP (Hartman and Vale, 1999). Katanin has been implicated in the organization of microtubule arrays in vivo and is required for assembly of the meiotic spindle in *Caenorhabditis elegans* (Srayko et al., 2000; McNally et al., 2006). Surprisingly, katanin deficiency led to a decrease in the microtubule polymer mass in the meiotic embryo of *C. elegans*, probably because severing generates microtubule fragments that serve as seeds for nucleation of new microtubules (Srayko et al., 2006). Katanin was also implicated in generation of short microtubules destined for transport to neural extensions (Baas et al., 2005). In plants, katanin is required for normal assembly of cortical bundles (Bichet et al., 2001; Burk et al., 2001). Furthermore, p80, the noncatalytic subunit of katanin, is required for assembly of central pair microtubules in ciliary axonemes of *Chlamydomonas reinhardtii* (Dymek et al., 2004). Thus, katanin has emerged as a positive regulator of the microtubule polymer mass, which is critical for assembly of diverse microtubule arrays.

On the other side, katanin activity increases during the mitotic prophase, suggesting that severing plays a role in the disassembly of interphase microtubules, to allow for reassembly of tubulin into the mitotic spindle (McNally and Thomas, 1998). Thus, katanin could also function as a negative regulator of the microtubule mass. The net effect of katanin on the polymer mass could depend on the size of microtubule products that are released by severing. Katanin could negatively regulate the polymer mass if the product of severing is a tubulin dimer or a short microtubule that cannot seed assembly.

Here, we show that katanin plays a negative regulatory role in the management of nonciliary microtubules in *Tetrahymena*. We show that katanin reduces the polymer mass as well as increases the level of polymer dynamics in the cell body. However, in the same cell, katanin promotes assembly of ciliary microtubules, and therefore its effects are microtubule-type specific. We also show that katanin-mediated severing is nonrandom

Correspondence to Jacek Gaertig: jgaertig@cb.uga.edu

R.C. Davis' present address is Department of Biochemistry and Molecular Biology, Colorado State University, Fort Collins, CO 80523.

Abbreviations used in this paper: LM, longitudinal microtubule bundle; PTM, post-translational modification; TEM, transmission electron microscopy.

The online version of this article contains supplemental material.

The Journal of Cell Biology, Vol. 178, No. 6, September 10, 2007 1065–1079
http://www.jcb.org/cgi/doi/10.1083/jcb.200704021

in vivo and that its activity is required to inhibit accumulation of post-translational modifications (PTMs) on microtubules. Furthermore, katanin mutations phenocopy a mutation of the domain of β-tubulin involved in polymeric PTMs, glutamylation (Eddé et al., 1990) and glycylation (Redeker et al., 1994). We propose that katanin regulates the longevity of nonciliary microtubules by preferentially depolymerizing post-translationally modified segments of the polymer.

Results

Katanin is required for disassembly of cell body microtubules and assembly of motile cilia in *Tetrahymena*

To identify microtubule-severing factor genes in *Tetrahymena thermophila*, we searched the recently sequenced genome of this ciliate for sequences encoding AAA type ATPases. We identified two sequences encoding a p60 katanin subunit, representing the predicted genes *KAT1* and *KAT2*, and a sequence encoding a spastin-like protein, *SPA1*. Spastin is a related ATPase with a microtubule-severing activity (Hazan et al., 1999; Roll-Mecak and Vale, 2005). The predicted Kat1p, Kat2p proteins have an AAA domain, but Kat2p also has an N-terminal LisH domain (Fig. 1 A). Kat1p and Kat2p belong to conserved clades and Kat1p is more closely related to the well-studied vertebrate p60s (Fig. 2). The *Tetrahymena* genome also contains a sequence encoding p80, the putative noncatalytic subunit of katanin, *KAT3*.

To evaluate the role of microtubule severing in vivo, we constructed strains lacking either *KAT1*, *KAT2*, *KAT3*, or *SPA1*. *Tetrahymena* has two nuclei: the germline micronucleus, and the somatic macronucleus. The macronuclear genome determines the phenotype. Heterokaryon strains were constructed that were homozygous for gene disruption in the micronucleus and had wild-type genes in the macronucleus. Heterokaryons have a wild-type phenotype during vegetative propagation, but when two such cells conjugate, they produce progeny cells with a new macronucleus that express a gene disruption phenotype. Heterokaryon progeny cells lacking either *KAT2* or *SPA1* had a normal morphology (see Fig. S3, available at http://www.jcb.org/cgi/content/full/jcb.200704021/DC1) and gave rise to clones with normal vegetative growth rates (Fig. S4 I). While 95% of control mating pairs gave rise to vigorous clones that grew to maximal cell density in drops ($\sim 10^6$ cells/ml), the isolated *KAT1* knockout heterokaryon pairs produced on average only 12 cells per mating pair ($n = 60$) and thus had divided completely only 2–3 times. After the initial complete cell cycles (presumably resulting in depletion of parental Kat1p), the *KAT1*-null cells underwent 1–3 incomplete cell cycles during which cells grew in size, the nuclei had divided, but the cleavage furrow did not complete its ingression. This led to the formation of multinucleated cell chains composed of cortical "subcells" (Fig. 3 A). In a wild-type vegetatively growing population, 97% of cells are composed of a single subcell and 3% have 2 subcells (cells undergoing cytokinesis). At 40 h (after mixing of heterokaryons), 90% of Kat1p-null cells were composed

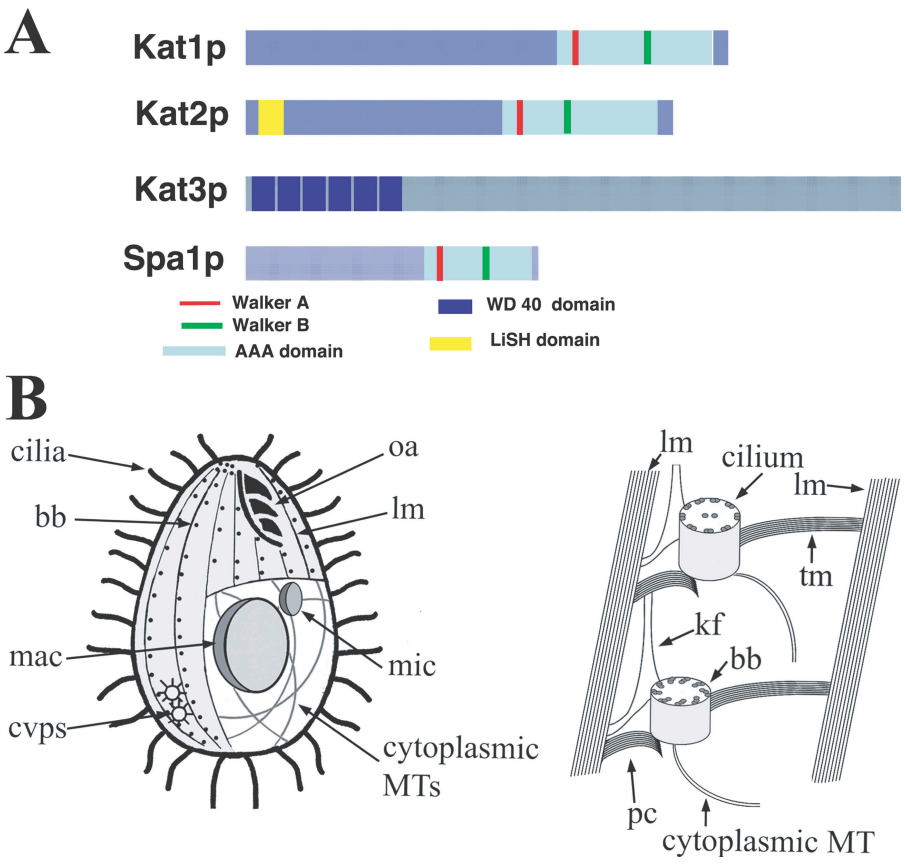

Figure 1. ***Tetrahymena* cytoskeletal organelles and domain organization of katanin subunits and spastin-like protein.** (A) Domain organization of predicted katanin- and spastin-like subunits of *Tetrahymena*. (B) Schematic drawings showing the main cytoskeletal organelles of *Tetrahymena*. Abbreviations: oa, oral apparatus; bb, basal body; lm, longitudinal microtubule bundle; mic, micronucleus; mac, macronucleus; tm, transverse microtubule bundle; pc, postciliary microtubule bundle; kf, kinetodesma (nonmicrotubular fiber); cvps, contractile vacuole pores.

of 2–4 subcells and had on average 2.7 subcells/chain ($n = 172$) (Fig. 4 D). Thus, the absence of zygotic Kat1p leads to an arrest in cytokinesis.

In *Tetrahymena* there are two distinct modes of nuclear division: the micronucleus undergoes mitosis at an early stage of cell division, while the macronucleus divides by amitosis (a microtubule-dependent nuclear division that does not involve chromatin condensation) at the time of cytokinesis. The subcells of *KAT1*-null cell chains contained a macronucleus and a micronucleus, indicating that the nuclear divisions and segregation of nuclei are not disturbed (Fig. 3 A). Thus, both mitosis and amitosis are insensitive to the levels of Kat1p. The *KAT1*-null cell chains remained viable for 3–4 d. However, no proliferating clones were obtained from mass matings of 2×10^7 *KAT1* knockout heterokaryons using paromomycin selection that eliminates nonprogeny cells (see Materials and methods). Thus, Kat1p is essential. Although Kat1p is not required for nuclear divisions, its activity is required for completion of cytokinesis.

During cytokinesis of wild-type *Tetrahymena* cells, cortical longitudinal microtubule (LM) bundles (see Fig. 1 B) undergo partial depolymerization within the equatorial region as the contractile ring ingresses. In the advanced stage *KAT1*-null cell chains labeled with anti-tubulin antibodies, LMs appeared thicker then normal. While some LMs are twisted and show gaps in the contraction areas, other LMs continued to span adjacent subcells despite the completion of nuclear divisions (Fig. 4 C, arrows). Because LMs are the only microtubule bundles that run perpendicularly to the cleavage furrow, we speculate that in the absence of katanin, some cortical LMs do not depolymerize properly at the time of cytokinesis and physically obstruct the ingressing cleavage furrow.

Within the cell body, cell chains lacking zygotic Kat1p had an abnormally dense network of intracytoplasmic microtubules. Quantitative immunofluorescence detected about twofold increase in the mass of insoluble tubulin in the cell body of *KAT1*-null cell chains, which indicates that the density of internal cytoplasmic microtubules increases in the absence of zygotic Kat1p (Fig. 5). Furthermore, the internal microtubules of *KAT1*-null mutants are hyperstable and excessively modified post-translationally (see below).

While wild-type *Tetrahymena* swim rapidly due to the beating of cilia, the *KAT1* knockout cell chains were nearly paralyzed. Immunofluorescence showed that the mutant cell chains had two types of cilia: a few normal-length cilia that were more abundant near the ends of cell chains, and a majority of excessively short cilia (Fig. 4, B and C; see Fig. 9, E and F). In the ciliary rows that cover the cell surface of *Tetrahymena*, new cilia-templating basal bodies form near old basal bodies, and old cilia are not resorbed (Allen, 1969). Most likely, the normal-length cilia are parental units, while the short cilia were assembled in the absence of zygotic Kat1p. The pattern of normal-length cilia in the *KAT1*-null cell chains is consistent with the known preference for insertion of new basal bodies within the mid-posterior region (Frankel et al., 1981; Thazhath et al., 2004). Transmission electron microscopy (TEM) showed that mutants lacking zygotic Kat1p assemble incomplete axonemes. Although all ciliary cross sections analyzed in wild-type cells had a 9+2 axoneme ($n = 55$) (Fig. 6 A), 80% of mutant cross

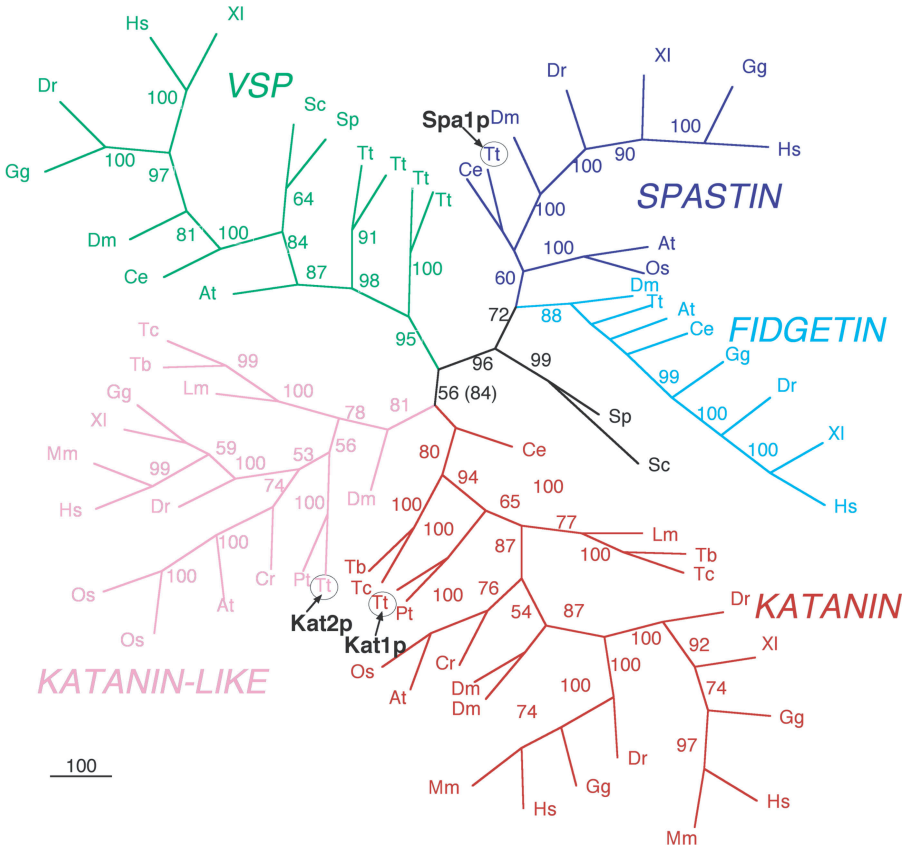

Figure 2. **Phylogeny of AAA domain proteins based on the sequence alignment shown in Fig. S1.** Numbers above branches represent bootstrap values above 50%. Abbreviations: At, Arabidopsis *thaliana*; Ce, *Caenorhabditis elegans*; Cr, *Chlamydomonas reinhardtii*; Dm, *Drosophila melanogaster*; Dr, *Danio rerio*; Gg, *Gallus gallus*, Hs, *Homo sapiens*; Lm, *Leishmania major;* Mm, *Mus musculus*; Os, *Oryza sativa*; Sc, *Saccharomyces cerevisiae*; *Tb, Trypanosoma brucei*; Tc, *Trypanosoma cruzi*; Tt, *Tetrahymena thermophila*; Xl, *Xenopus laevis*. Fig. S1 is available at http://www.jcb.org/cgi/content/full/jcb.200704021/DC1.

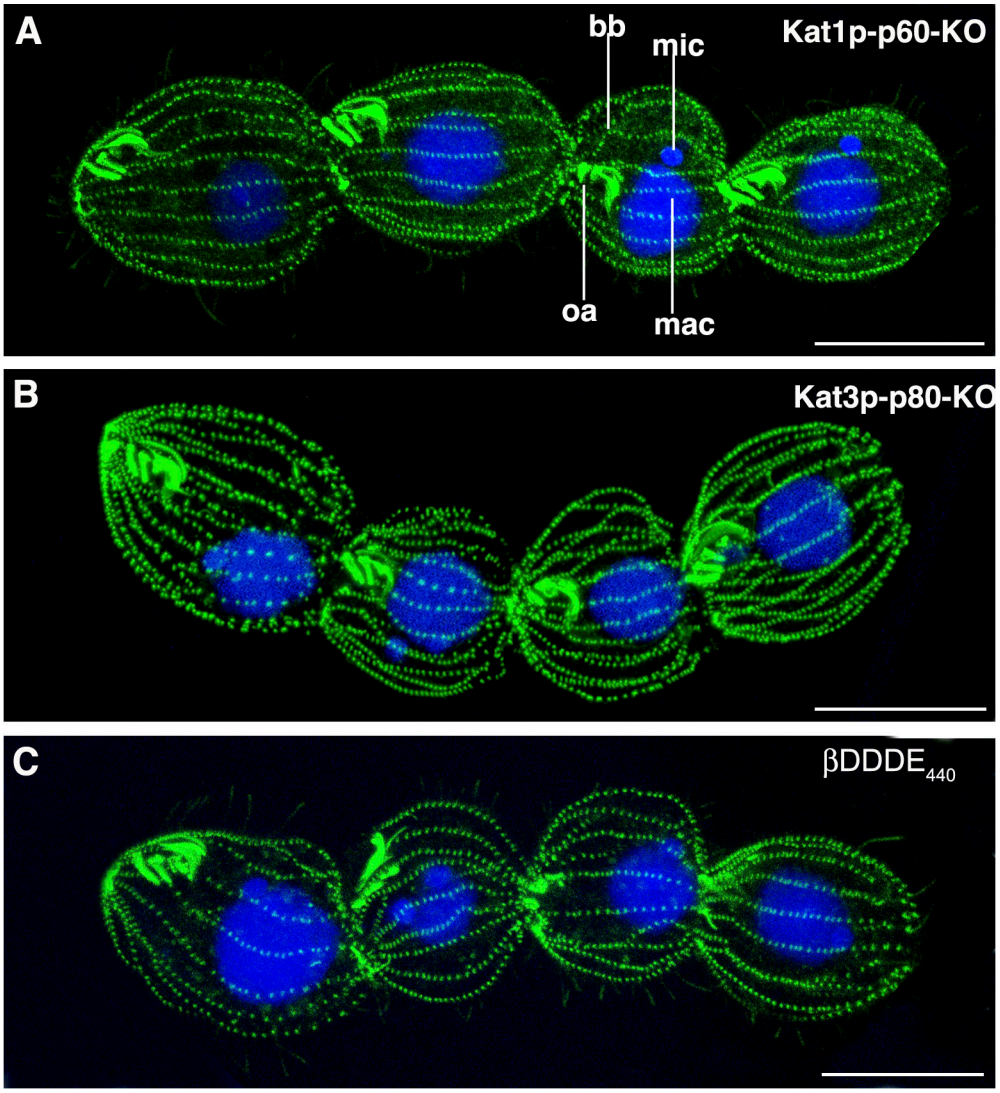

Figure 3. **The katanin subunit null mutations phenocopy the βDDDE$_{440}$ mutation on β-tubulin that inactivates sites of polymodifications.** Mutant cells (obtained from matings of appropriate heterokaryons) were immunolabeled with an anti-centrin antibody and co-stained with DAPI. (A) A mutant cell lacking zygotic Kat1p (p60). (B) A mutant cell lacking zygotic Kat3p (p80). (C) A βDDDE$_{440}$ mutant cell chain. Abbreviations: mac, macronucleus; mic, micronucleus; oa, oral apparatus; bb, basal body. Note that nuclei divide and segregate, but cells fail cytokinesis multiple times. Bars, 50 μm.

sections (n = 205) had peripheral doublets (associated with radial spokes and dynein arms) but lacked a central pair (9+0) (Fig. 6, B and C). The remaining 20% of normal 9+2 cross sections most likely represent cilia assembled before depletion of Kat1p.

In other organisms, katanin functions as a complex of p60 and p80, a noncatalytic subunit (McNally and Vale, 1993; Srayko et al., 2000). The progeny of heterokaryons lacking the *KAT3* (p80) gene developed into paralyzed cell chains that were remarkably similar to those produced by the lack of *KAT1* (Fig. 3 B and unpublished data). The simplest explanation is that Kat1p and Kat3p work in the same pathway, and both are required for katanin activity.

Importantly, a strikingly similar paralyzed cell chain phenotype (with 9+0 axonemes) was earlier observed for the βDDDE$_{440}$ mutation of β-tubulin (Fig. 3 C and Fig. 4 D). This mutation inhibits acquisition of polymeric PTMs, glutamylation and glycylation on the C-terminal tail of β-tubulin (Thazhath et al., 2002, 2004). Thus, katanin and polymodifications on β-tubulin could function in the same pathway.

Kat1p (p60) has selective microtubule-severing activity in vivo

To test whether Kat1p has a microtubule-severing activity, we overproduced GFP-Kat1p using an inducible promoter at high copy number. After induction, GFP-Kat1p accumulated in cells (Fig. 7 A) and cell multiplication was inhibited (Fig. 7 D). After 2–7 h, overproducing cells had fewer microtubules based on a decrease in the immunofluorescence signal of polymerized tubulin (unpublished data). Nearly all microtubules disappeared after 12 h (Fig. 7 B). We were intrigued by the rapid loss of ciliary axonemes (Fig. 7, B and C) because katanin was earlier implicated in deciliation, a rapid shedding of cilia caused by low pH, based on severing of outer doublets at the transitional zone

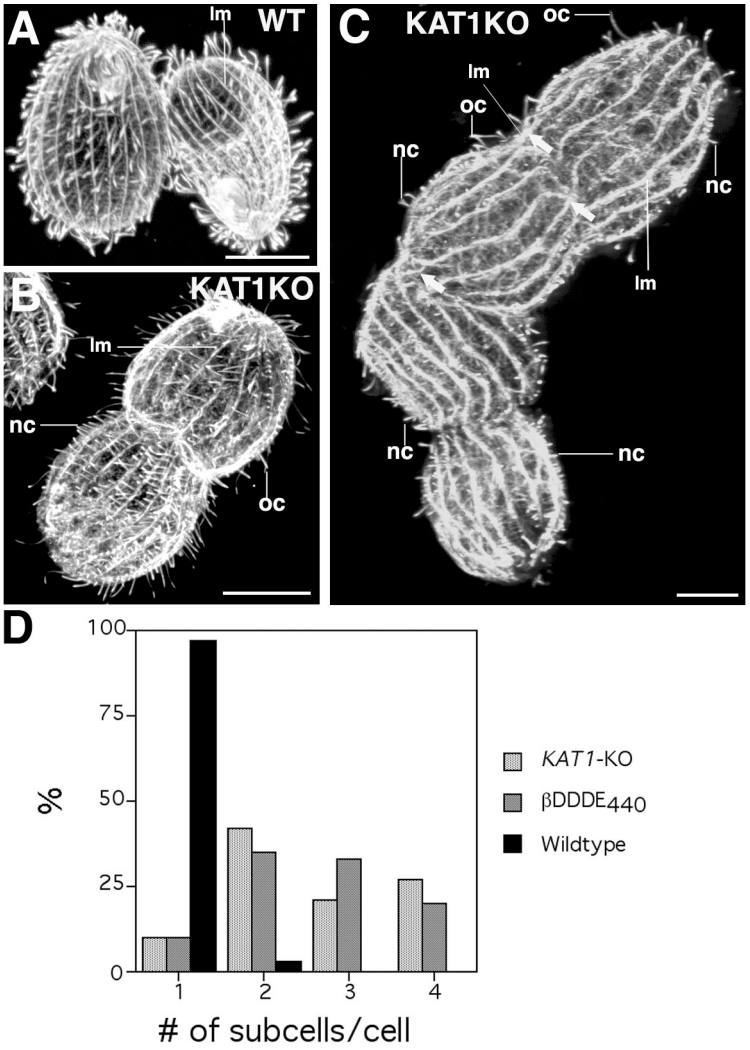

Figure 4. **Cells lacking zygotic Kat1p assemble excessively short cilia and have thickened cortical microtubule bundles (LMs).** Cells were labeled for α-tubulin using the 12G10 antibody. (A) Wild type. (B) An early-stage cell chain lacking zygotic Kat1p composed of two subcells. (C) A late-stage Kat1p-null cell chain composed of four subcells. Note an increase in the thickness of LM bundles as the mutant cell continues to grow while failing cytokinesis (compare with B). Although some LMs are broken in the cleavage furrow area, some LMs (arrows) appear to be continuous across subcells, indicating a failure in their depolymerization during cytokinesis. (D) Quantification of cell morphology in wild-type, *KAT1*-null, and $\beta DDDE_{440}$ mutants 40 h after mating of heterokaryons. The fractions of cells with specific numbers of subcells were determined and are shown as percentages ($n = 100$ for wild type, $n = 172$ for *KAT1*-null, $n = 305$ for $\beta DDDE_{440}$). Abbreviations: *nc*, newly assembled short cilia; *oc*, preexisting (old) cilia; *lm*, longitudinal microtubule bundles. Bars, 20 μm.

(Lohret et al., 1998; Quarmby, 2004). TEM showed that many cilia of GFP-Kat1p–overproducing cells had severed axonemes, but in all cases analyzed the breakage points were present outside of the transitional zone (Fig. 6, D–G). 44% ($n = 91$) of TEM cross sections of cilia in GFP-Kat1p–overproducing cells lacked one or more outer doublet microtubule profiles (Fig. 6, I–M), whereas 21% of cross sections had singlet peripheral microtubules, indicating a selective loss of the entire B-tubule (Fig. 6, N and O). Strikingly, on most cross sections the central pair microtubules were intact (Fig. 6, H–O). Thus, the A-tubule of the doublet and the central microtubules are either less accessible or more resistant to severing by overproduced katanin. Importantly, 31% of ciliary cross sections ($n = 91$) had two axonemes profiles adjacent to each other (Fig. 6, H–M). In most of these cilia, one axoneme profile was more fragmented. In one case only the central pair and a single singlet peripheral microtubule were present in the axoneme fragment (Fig. 6 M). All these images collectively suggest a likely mechanism of loss of ciliary axonemes in GFP-Kat1p–overproducing cells. Initially, one or more of the outer doublets could undergo nicking, introducing a point of structural weakness, and the beating of cilia could break the axoneme (Fig. 6, D–G). Next, the distal portion of the axoneme could slide past the proximal portion. The residual axoneme and the broken fragment could undergo further fragmentation (Fig. 6, F, G, and J–M).

Overexpressed GFP-Kat1p also affected the triplet microtubules of basal bodies. By inspecting the undulating membrane (UM) of the oral apparatus, we found additional signs of selectivity in the GFP-Kat1p–severing activity. In the UM, the basal bodies are arranged into two rows with the same orientation, with only the outer row being ciliated. Strikingly, only the basal bodies of the outer row showed defects and the affected triplets were located at the same circumferential positions in adjacent organelles (Fig. 6 P). Thus, Kat1p is a genuine severing protein, but the enzyme has preferred sites of activity on a subset of microtubules in vivo.

Overproduction of either Spa1 or Kat2p GFP fusions did not affect the multiplication rate or organization of microtubules (Fig. S4, A–H and J).

GFP-Kat1p localizes to basal bodies, LMs, and axonemal microtubules

Attempts at generating polyclonal antibodies against Kat1p were unsuccessful. We tagged Kat1p with GFP by rescuing

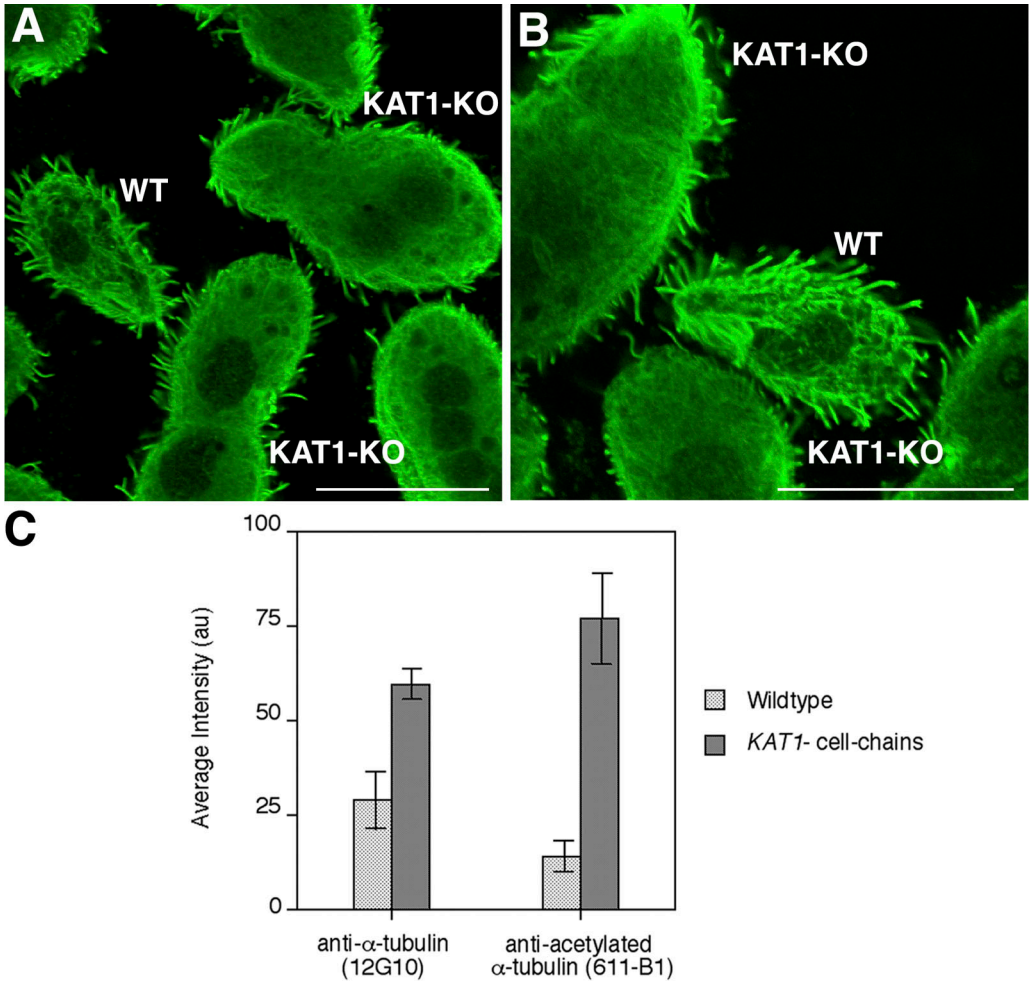

Figure 5. **Cells lacking zygotic Kat1p have increased levels of polymerized tubulin in the cell body.** (A and B) Mutant and wild-type cells were mixed, detergent extracted, and processed for immunofluorescence using 12G10 anti–α-tubulin. Internal confocal sections are shown. Note an increased tubulin signal in the mutant cell chains. (C) Results of quantitative immunofluorescence using a general anti–α-tubulin antibody (12G10) and 6–11 B-1, an anti-acetylated K-40 α-tubulin antibody. Wild-type and mutant cell chains that were laying side-by-side on the same confocal optical sections were imaged. Internal sections were chosen and 100 average pixel values were determined for randomly chosen rectangular areas for 10 different mutant and adjacent wild-type cells. Bars, 50 μm.

progeny of *KAT1* heterokaryons, with a GFP-KAT1 gene targeted to the native locus. However, the rescue strains did not have detectable GFP expression (based on Western blotting and immunofluorescence with anti-GFP antibodies; unpublished data). Thus, the native promoter-driven Kat1p could be below the detection limit. Next, we rescued mating *KAT1* heterokaryons with a fragment encoding GFP-Kat1p under the control of a cadmium-dependent promoter maintained at a low copy number (see Materials and methods). The GFP-Kat1p rescue strains grew more slowly in the absence of exogenous cadmium, but had a normal rate of multiplication with cadmium (Fig. 8 A). In immunolabeling with anti-GFP antibodies, GFP-Kat1p was detected near the basal bodies (Fig. 8 B). In fixed cells that were not processed for immunofluorescence, we also detected GFP-Kat1p fluorescence as lines on a side of rows of basal bodies (Fig. 8 C), indicating that GFP-Kat1p also associates with LMs (see Fig. 1 B). Thus, light microscopy studies detected GFP-Kat1p in the cell cortex (near basal bodies and along LMs) but not inside cilia. However, using post-embedding immunogold EM we detected GFP-Kat1p epitopes in two locations: near the basal bodies (Fig. 8 D, a and b) and within cilia. Strikingly, GFP-Kat1p was seen exclusively near the outer doublets and not near the central pair (Fig. 8 D, c–e). Although control ciliary sections of wild-type cells lacked gold particles ($n = 25$), 71% of sections of cilia in GFP-Kat1p–expressing cells were labeled, and in all cases the particles were found near the outer doublets ($n = 51$).

Lack of katanin stimulates microtubule PTMs

Our observation that katanin-null mutations phenocopy a β-tubulin polymodification domain mutation (Fig. 3 and Fig. 4 D) opened a possibility that katanin interacts with post-translationally modified microtubules. To further explore the relationship between microtubule PTMs and katanin, we examined the levels of specific PTMs in the Kat1p-null cells. In wild-type cells, tubulin polymodifications (glutamylation and glycylation) are present on most microtubules. However, on the relatively

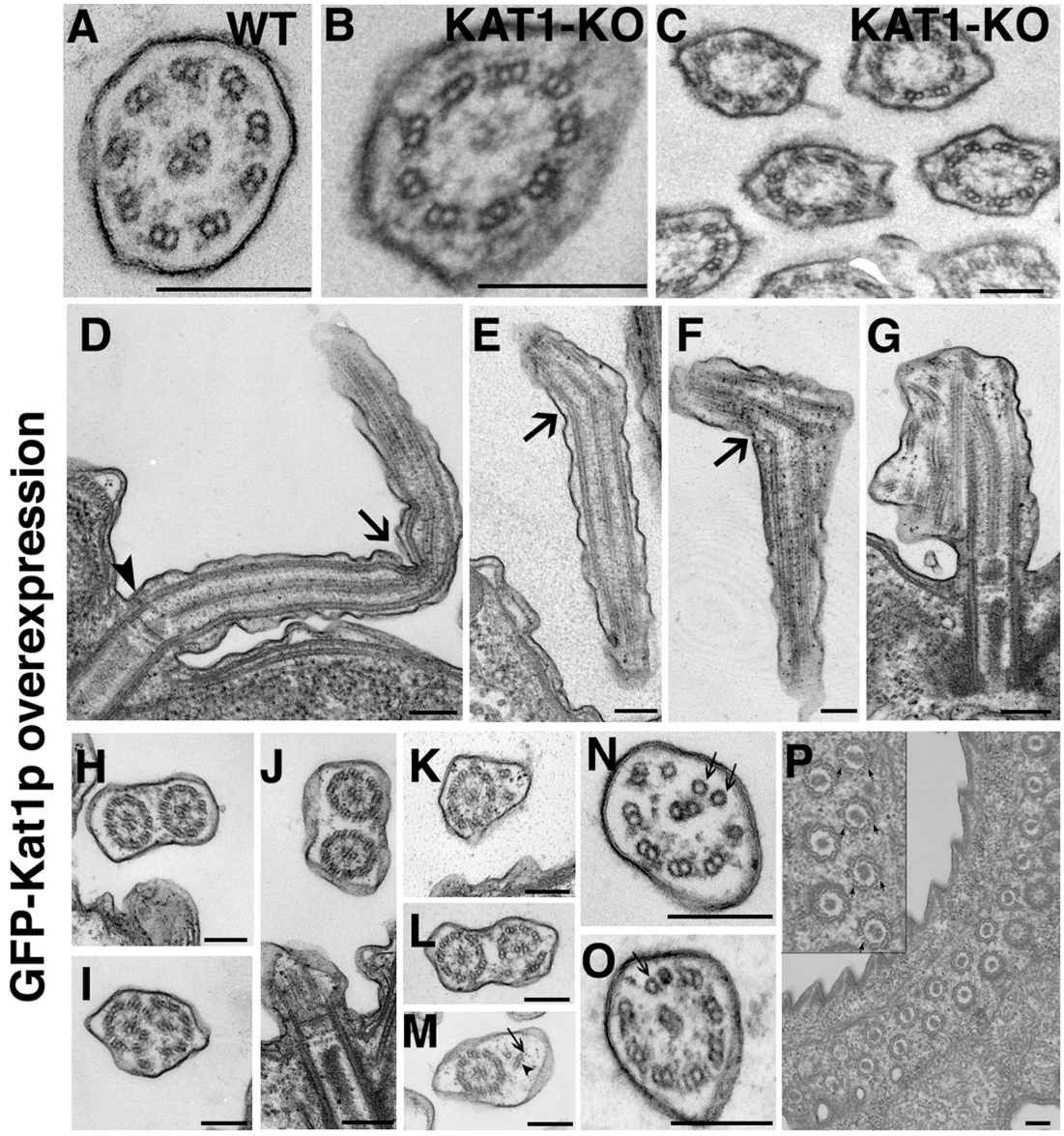

Figure 6. **Kat1p is required for assembly of 9+0 cilia and overexpression of GFP-Kat1p disassembles cilia.** (A–C) Lack of Kat1p katanin p60 induces 9+0 cilia. TEM cross sections of wild-type (A) and Kat1p-null mutant (B and C) cilia. C contains a section of multiple cilia of a developing membranelle of an oral apparatus. Note that mutant cilia lack the central pair of microtubules while the doublet microtubules with dynein arms and radial spokes are present. (D–P) Excessive GFP-Kat1p nicks and severs axonemal microtubules in vivo. TEM images obtained for *Tetrahymena* cells that overproduced GFP-Kat1p after induction with cadmium chloride for 2–6 h. (D–G) Longitudinal sections of axonemes in different stages of breakage and translocation of the distal part. Note that the transitional zone (arrowhead) does not show signs of severing. (H–M) Cross sections of cilia showing two axoneme profiles that positioned side by side. For K–M note that one axoneme fragment (probably distal in origin, see G) shows more extensive depolymerization of doublets, but the central pair remains stable. M shows a case where the distal axoneme fragment that translocates lacks all doublets except one, but still has a central pair. (N–O) Cross sections of axonemes showing doublets missing the B-tubule (arrows). (P) A cross section of an oral undulating membrane at the level of basal bodies. Note that some triplet microtubules are partly depolymerized to doublets or singlets (arrows in inset). Note that the affected triplets are severed at precisely the same circumferential positions in different basal bodies. All bars represent 0.2 μm, except in panel P where bar is 0.25 μm.

dynamic internal microtubules, the side chains are limited to a single G (Xia et al., 2000) or E (unpublished data). To evaluate the effect of Kat1p on the pattern of polymodifications, we used antibodies that recognize side chains with three or more units (ID5 for polyglutamylation (Rudiger et al., 1999) and AXO49 for polyglycylation (Levilliers et al., 1995)) for immunofluorescence. Although all wild-type cells analyzed lacked internal polymodified microtubules ($n = 58$), most *KAT1*-null cell chains had detectable polyglycylated and polyglutamylated internal microtubules in the cell body (56% [$n = 48$] and 75% [$n = 65$], respectively) (Fig. 9, B and C). In the cell cortex of wild-type cells, polyglutamylation is detectable only in basal bodies and cilia (Fig. S2 C, available at http://www.jcb.org/cgi/content/full/jcb.200704021/DC1), whereas cortical bundles are only monoglutamylated (unpublished data). However, in most *KAT1*-null cell chains, cortical LMs were labeled with an anti-polyglutamylation antibody (Fig. S2 D). All cortical microtubules (basal bodies, transverse microtubule bundles,

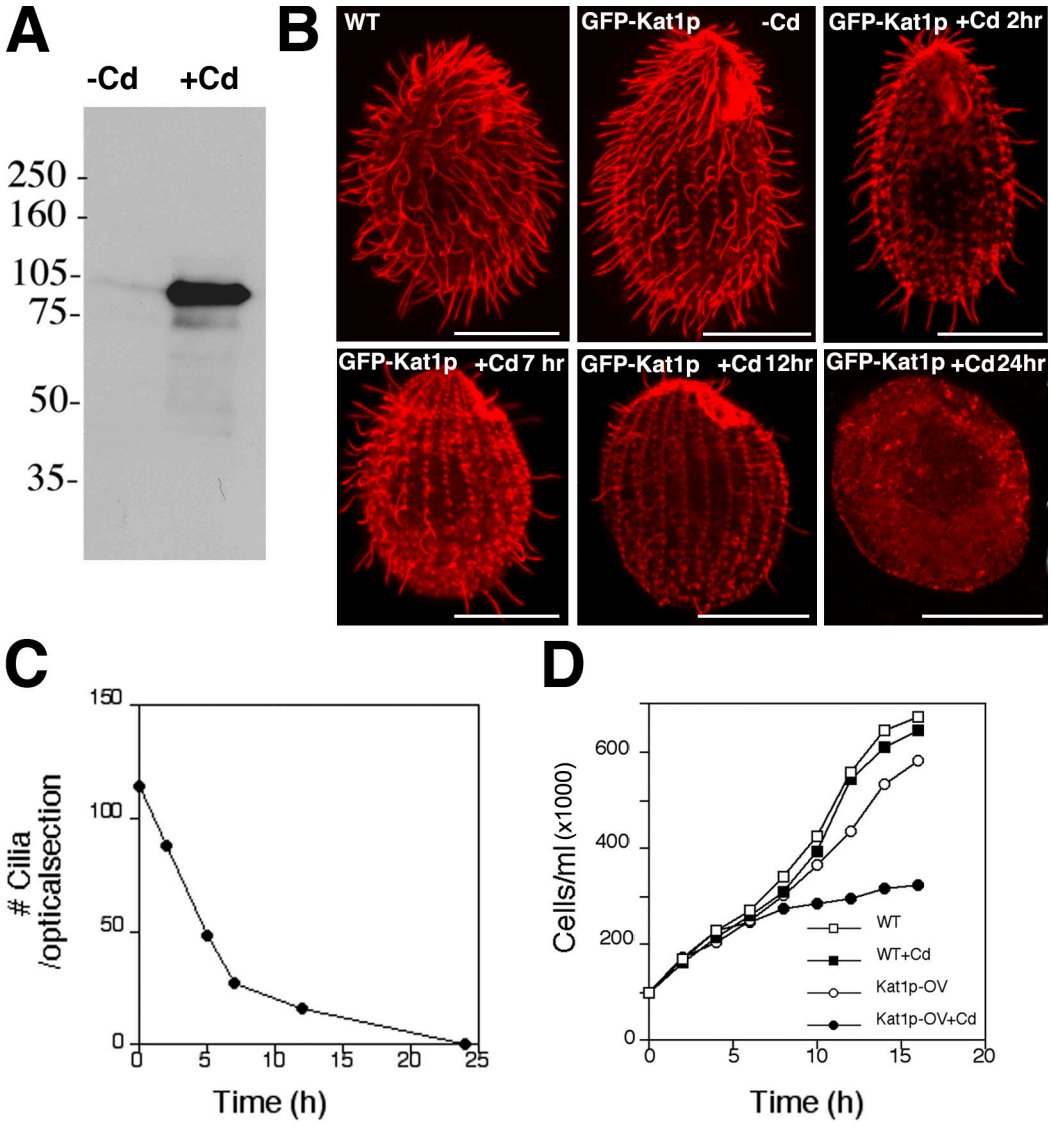

Figure 7. **Excessive GFP-Kat1p causes massive loss of microtubules in vivo.** (A) A Western blot shows accumulation of GFP-Kat1p in overproducing cells. Total cell protein was obtained from transformed cells carrying a GFP-Kat1p encoding gene under control of the *MTT1* promoter at high copy number that either were treated or not with 2.5 μg/ml cadmium chloride for 3 h. The blot was reacted with anti-GFP antibodies. (B) Confocal images of cells labeled by immunofluorescence using 12G10 anti-α-tubulin. The cell shown in the top left corner is a wild-type control treated with cadmium. The cell in the middle in the top row is a GFP-Kat1p transgene-carrying cell, which was not exposed to exogenous cadmium. The remaining cells were treated with cadmium chloride for 2–24 h. Note progressive loss of microtubular structures including cilia and basal bodies. Bars, 20 μm. (C) A graph that illustrates the rate of loss of cilia in response to accumulation of GFP-Kat1p. (D) A graph that shows the deleterious effect of GFP-Kat1p overproduction on multiplication of *Tetrahymena*. Either wild-type or transgenic cells carrying GFP-KAT1 coding region under *MTT1* promoter at high copy number (Kat1p-OV) were grown with and without exogenous cadmium. Note that cadmium alone does not affect wild-type cells.

and post-ciliary microtubule bundles; see Fig. 1 B) were labeled with the AXO49 anti-polyglycylation antibody in both wild-type and *KAT1*-null cells (unpublished data). Thus, based on the pattern of antibody labeling, we could not determine whether a polyglycylation side chain lengthening has occurred in the absence of Kat1p.

In wild-type cells, an assembling short cilium labels strongly with an anti-polyglutamylation antibody ID5, but the signal decreases as the cilium elongates and matures. The anti-polyglycylation antibody AXO49 gives a complementary pattern with a higher signal in mature cilia compared with short assembling cilia (Fig. 9 D). In the *KAT1*-null cell chains, the short cilia (presumably assembled in the absence of zygotic Kat1p) had higher level of polyglutamylation and lower level of polyglycylation as compared with normal-length cilia of parental origin concentrated mainly at cell extremities (Fig. 9, E and F). Thus, based on the pattern of microtubule PTMs, the cilia assembled in the absence of zygotic Kat1p resemble immature normal cilia. Although the pattern of polymodifications on most cilia in KAT1-null cells is abnormal, it is unclear whether katanin directly affects the levels of PTMs on ciliary microtubules or affects another process that is required for elongation and maturation of cilia.

In *Tetrahymena*, the internal cytoplasmic microtubules are dynamic, judged by their sensitivity to microtubule-depolymerizing compounds (Stargell et al., 1992) and lack of K-40 α-tubulin

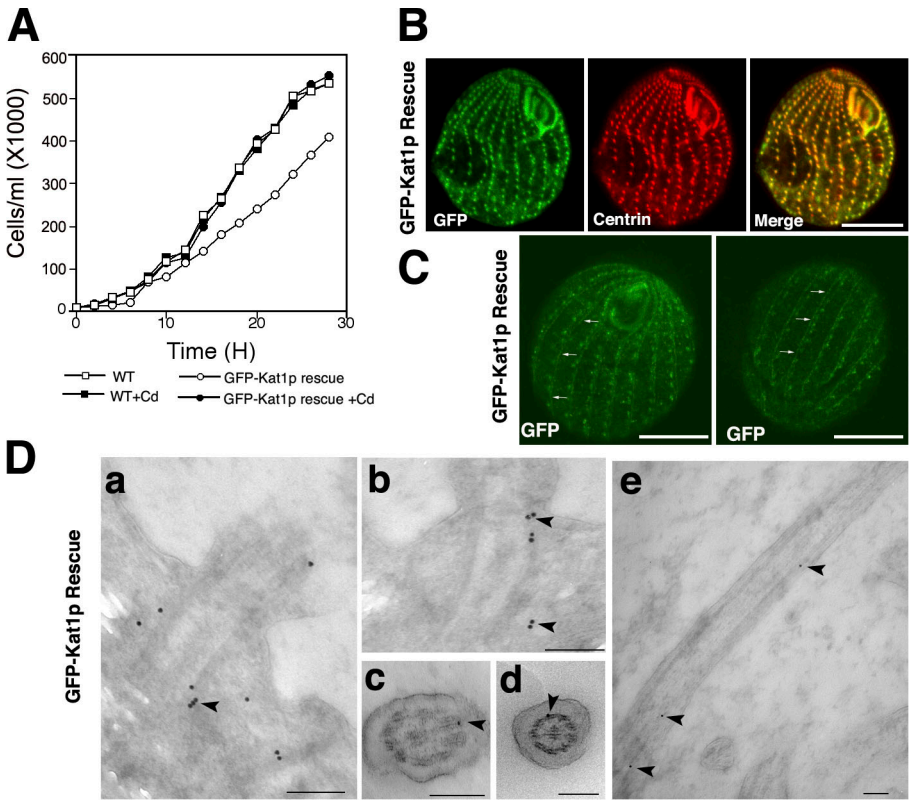

Figure 8. **GFP-Kat1p overexpressed at a moderate level does not affect cell multiplication and localizes to a subset of microtubules.** (A) A graph shows the rates of cell multiplication of a wild-type and GFP-Kat1p (low copy) rescue strain with and without exogenous cadmium. Note that the rescue strains grow more slowly without cadmium, presumably because an uninduced *MTT1* promoter is not expressed at a level that supports normal growth rate. However, the rescue strain grows normally with cadmium. (B) Confocal images showing that GFP-Kat1p (direct GFP signal) colocalizes with basal bodies that were colabeled with anti-centrin antibodies. (C) Confocal images of GFP-Kat1p rescue cells that were fixed with paraformaldehyde. Note that in addition to dots of fluorescence that correspond to the basal bodies, GFP-Kat1p is present as a line on one side of dots (arrows), consistent with the location of LM cortical bundles (see Fig. 1 B). (D) Immunogold (post-embedding) study reveals the presence of GFP-Kat1p in association with basal bodies (a and b) and outer doublets in cilia (c–e). To reduce the possibility of mislocalization, we used noninduced GFP-Kat1p rescue cells (not treated with cadmium) for immunogold TEM. All bars represent 0.25 μm, except in D (c–e) where bars are 0.2 μm.

acetylation (a marker of stable microtubules [Piperno et al., 1987]). Strikingly, based on immunofluorescence with the 6–11 B-1 antibody that recognizes α-tubulin acetylated at K-40, the Kat1p-null cell chains had strong acetylation on the internal cytoplasmic microtubules (Fig. 9 A). Although all wild-type cells analyzed did not have detectable acetylated internal microtubules ($n = 50$), such microtubules were detected in 99% ($n = 76$) of *KAT1*-null cell chains. Using quantitative immunofluorescence, a severalfold increase in the signal of acetylated tubulin was detected in the cell body of cell chains (Fig. 5 C). A Western blot of total cell chains (Fig. 9 G) showed levels of tubulin acetylation similar to wild-type cells, but cell chains have excessively short cilia and therefore lack a major source of acetylated tubulin that wild-type cells have (Gaertig et al., 1995). Thus, the Western blot result is consistent with an increase in acetylation on nonciliary microtubules in the absence of zygotic Kat1p. Cells lacking Kat3p (p80) also had hyperacetylated internal microtubules (unpublished data). However, elimination of either Kat2p or Spa1p did not lead to hyperacetylation of internal microtubules (Fig. S3, A–C). The accumulation of hyperacetylated microtubules is not an indirect consequence of absence of cytokinesis because cells blocked in cytokinesis by a distinct mechanism did not accumulate hyperacetylated cytoplasmic microtubules (Fig. S2, A and B). To summarize, a deficiency in katanin increases the levels of several PTMs on nonciliary microtubules. Specifically, internal microtubules show increased levels of glutamylation, glycylation, and acetylation, whereas cortical microtubules are hyperglutamylated in the absence of zygotic Kat1p. Thus, katanin functions as a negative regulator of microtubule PTMs in the cell body.

Katanin increases microtubule dynamics in vivo

Internal cytoplasmic microtubules of *Tetrahymena* depolymerize in the presence of nocodazole, whereas cortical and ciliary microtubules do not (Stargell et al., 1992). The accumulation of acetylation and polymodifications on internal microtubules in the Kat1p-null cell chains indicated that these microtubules were hyperstable. Indeed, after 1 h treatment with 40 μM nocodazole, all wild-type cells examined lacked detectable cell body microtubules ($n = 60$) (Fig. 10, A and C), whereas in 84% ($n = 75$) of Kat1p-null cell chains, cytoplasmic microtubules remained abundant (Fig. 10, B and D). Thus, the phenotype of *KAT1* deficiency could be caused to some extent by hyperstability of MTs. To test this hypothesis further, we incubated a population of *KAT1*-null cell chains with either 2 μM oryzalin or 10 μM paclitaxel to either destabilize or hyperstabilize MTs, respectively. Remarkably, oryzalin increased the number of complete cell divisions undergone by cells lacking zygotic Kat1p (Fig. 10 F). The treatment with paclitaxel blocked multiplication of Kat1p-null cells (Fig. 10 F). At these concentrations, neither of the drugs affected the growth of wild-type cells (Fig. 10 E). This pharmacological profile indicates that katanin-deficient cells have hyperstable microtubules and that katanin increases dynamics of microtubules in vivo.

Katanin is not required for deciliation in *Tetrahymena*

Deciliation is a rapid shedding of cilia in response to chemical stresses (e.g., low pH), based on breakage of the axoneme within the transitional zone. Katanin was implicated in severing of axonemes in *Chlamydomonas* (Lohret et al., 1998). Surprisingly, the

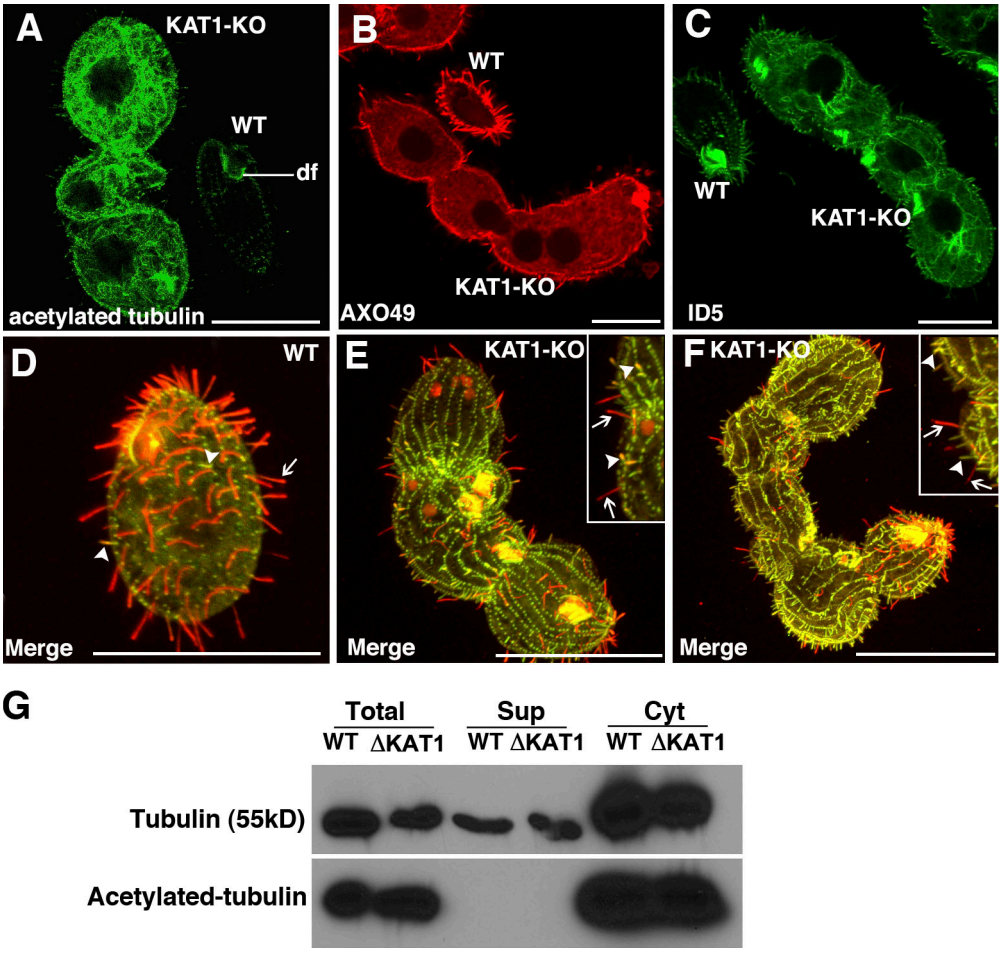

Figure 9. **Lack of zygotic Kat1p leads to accumulation of acetylated and polymodified microtubules in the cell body of *Tetrahymena*.** (A–C) Cell chains lacking zygotic Kat1p were mixed with wild-type cells and processed for immunofluorescence using the 6–11 B-1 anti-acetylated K-40 α-tubulin (A), AXO49 anti-polyglycylated tubulin (B), and ID5 anti-polyglutamylated tubulin (C) antibody. Single internal confocal optical sections of a mutant and an adjacent wild-type cell are shown. Note that wild-type cells lack internal acetylated, polyglycylated, and polyglutamylated microtubules in the cell body except for the acetylated oral deep fiber (df). (D–F) Composite confocal images of wild-type (D) and Kat1p-null (E and F) cells double-labeled for polyglycylation (red) and polyglutamylation (green). Note that in a wild-type cell, short developing cilia (arrowheads) show a low signal of polyglycylation and a strong signal of polyglutamylation, whereas a reverse relationship is observed for the majority of cilia that are mature (arrow). In the mutants (E and F) the majorities of cilia are short (arrowheads) and maintain an apparent high level of polyglutamylation and low level of polyglycylation as compared with normal length parental cilia (arrows). (G) A Western blot analysis of either wild type of a population highly enriched in cells lacking zygotic Kat1p. To prepare the mutant population, we mated *KAT1* heterokaryons *en masse*, re-fed cells after 24 h, and allowed the progeny to develop the mutant phenotype. We prevented the population from being overgrown by cells that failed to mate by adding paromomycin (progeny cells, but not cells that aborted conjugation, are resistant to paromomycin due to the expression of the *neo3* cassette). Either total cell (total) or soluble protein (sup) or cytoskeletons (cyt) after Triton X-100 extraction were loaded and probed with either 12G10 antibody (anti–α-tubulin) or 6–11 B1 (anti-acetylated Lys-40 on α-tubulin). The blot was first probed with anti-tubulin (top blot), then stripped off and re-probed with an anti-acetylated tubulin antibody (bottom blot). Note that the levels of soluble tubulin are similar in wild-type and mutant cells, indicating that katanin does not affect the size of the soluble tubulin pool. Also, the levels of acetylated tubulin in microtubules are similar. Given that mutant cells have excessively short cilia, there must have been an increase in the levels of acetylation in the cell body, consistent with immunofluorescence shown in panel A. Bars, 50 μm

Kat1p-null cell chains deciliated in low pH. Nearly all cilia were lost, indicating that the short cilia that assemble under katanin deficiency also shed (Fig. S5, A and B; available at http://www.jcb.org/cgi/content/full/jcb.200704021/DC1). The deciliated Kat1p-null cells regenerated uniformly short cilia within 2 h (Fig. S5 C) and remained paralyzed, indicating that the regenerated cilia were 9+0. Double-knockout cell chains lacking *KAT1* and *KAT2* also shed (Fig. S5, D and E) and regenerated cilia (unpublished data), indicating that in *Tetrahymena* deciliation is not dependent on p60 and p60-like proteins. Furthermore, the ability of katanin- deficient cells to regenerate cilia indicates that the absence of katanin does not lead to a general deficiency in the pool of unpolymerized tubulin in the cell body. This was confirmed by a Western blot that showed that cell chains had a normal level of soluble (Triton X-100 extractable) tubulin (Fig. 9 G).

Discussion

Katanin can act as a negative regulator of microtubule mass and dynamics

We have investigated the functions of katanin- and spastin-like proteins in *Tetrahymena thermophila*. The use of *Tetrahymena* enabled us to establish the significance of severing in a cell

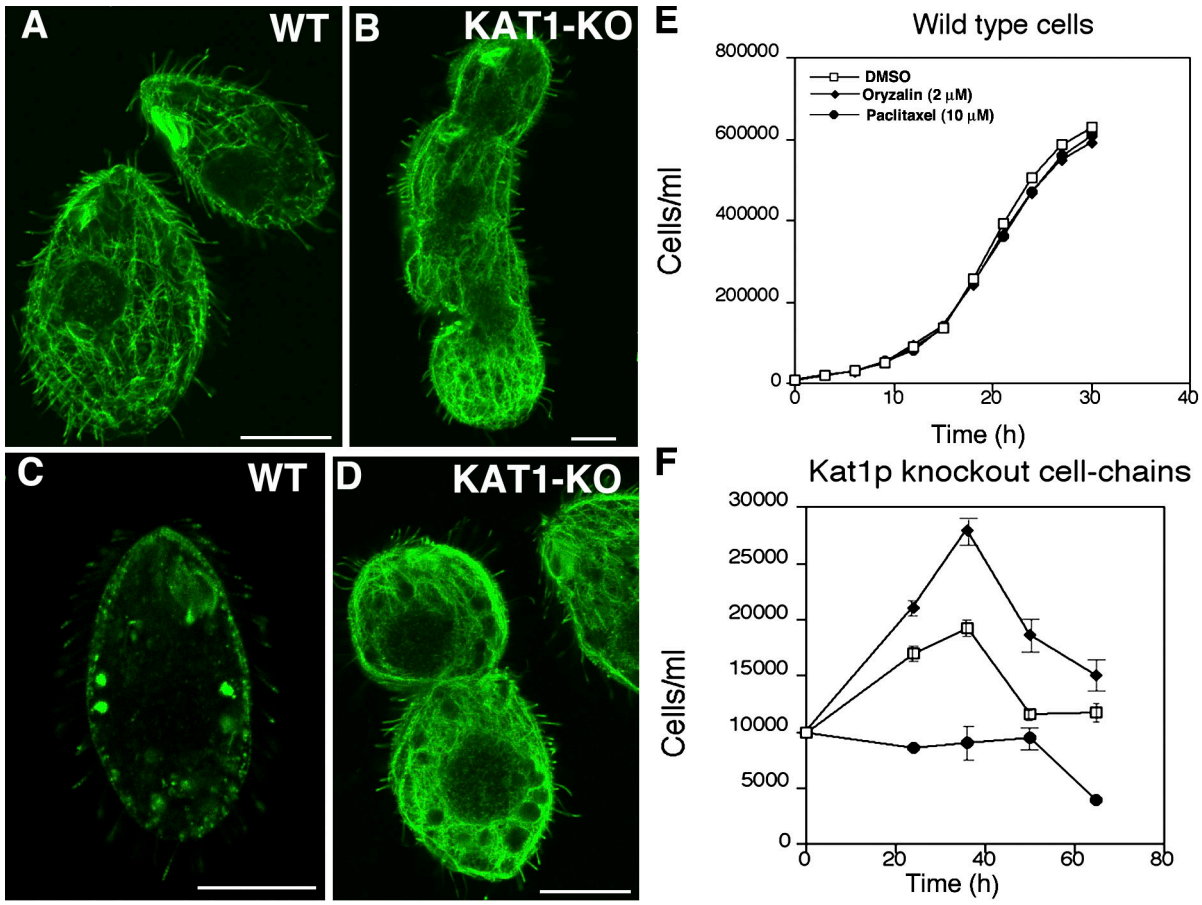

Figure 10. **Cytoplasmic microtubules in cells lacking zygotic katanin are hyperstable.** (A–D) Internal confocal optical sections of either wild-type cells (A and C) or cell chains lacking zygotic Kat1p (B and D) that were treated with DMSO as a solvent control (A and B) or 40 μM nocodazole (C and D) and processed for immunofluorescence using 12G10 anti–α-tubulin. Note that cytoplasmic microtubules depolymerized in the wild-type cell but are still abundant in the mutant. Bars, 20 μm. (E) The effect of either paclitaxel or oryzalin on the rate of multiplication in wild-type cells. (F) Cell multiplication in a population enriched in mutant cells after mass mating of *KAT1* heterokaryons, treated either with 2 μM oryzalin, 10 μM paclitaxel, or DMSO as a solvent control.

type with diverse microtubules, including those forming internal networks, cortical arrays, and axonemes. We show that the absence of spastin-like protein Spa1p, and katanin-like protein, Kat2p, does not detectably change the phenotype of vegetative *Tetrahymena* cells. It remains to be determined whether Kat2p and Spa1p play a role during conjugation, the sexual stage of ciliate life cycle. Furthermore, spastins are phylogenetically related to fidgetins and the *Tetrahymena* genome contains a single sequence encoding a fidgetin-like protein (Fig. 2). In light of the recent demonstration that fidgetin contributes to shortening of spindle microtubules during mitosis in *Drosophila* (Zhang et al., 2007), in the future, a potential functional redundancy between spastin and fidgetin will need to be addressed in *Tetrahymena*.

We show that katanin affects the microtubule polymer mass differentially depending on the intracellular location. Specifically, we show that katanin decreases the polymer mass of nonciliary internal microtubules, and increases the mass of ciliary microtubules. In *Caenorhabditis elegans* meiotic embryos, deficiency in katanin decreased the polymer mass, likely because in this cell type, katanin produces shorter microtubules that provide new free microtubule ends for polymerization (McNally et al., 2006; Srayko et al., 2006). The different outcome that we observed for the cell body of *Tetrahymena* can be reconciled with the *C. elegans* studies, if, in *Tetrahymena*, katanin releases tubulin dimers or short microtubules that cannot prime assembly. Thus, the consequences of katanin presence could depend on the size of severing products as well as on the cellular context that determines the fate of microtubule fragments. Interestingly, the consequences of the loss of spastin in other organisms were similar to what we observed in *Tetrahymena* for katanin. A mutation of murine spastin induced swellings in axons that were enriched in detyrosinated, stable microtubules (Tarrade et al., 2006). A knockdown of spastin mRNA in *Drosophila* caused stabilization of microtubules (Trotta et al., 2004; Orso et al., 2005), although another study reported a reduced number of microtubules in spastin-deficient *Drosophila* (Sherwood et al., 2004). Thus, most of the studies on spastin, collectively with our data, indicate that microtubule severing increases polymer dynamics and reduces PTMs on microtubules.

Katanin severs preferred microtubule sites in vivo

Our data indicate that katanin displays a high level of microtubule substrate selectivity in vivo. A moderately overproduced

GFP-Kat1p localized with only a subset of microtubule locations. We detected tagged Kat1p around the basal bodies, near LMs and doublet microtubules inside cilia. The basal body–associated katanin may be involved in severing of minus ends of internal cytoplasmic microtubules and may contribute to the dynamic character of these microtubules. Cortical LMs are bundles of partly overlapping microtubules with a uniform polarity (Pitelka, 1961). Katanin may be involved in the turnover of segment microtubules in LMs, and its deficiency could lead to abnormal persistence of LMs and block cytokinesis.

Although it is unclear whether katanin under physiological conditions severs stable microtubules of cilia and basal bodies, these structures were severed by an overproduced katanin. Remarkably, katanin preferentially severed microtubule triplets located at specific positions, confirming that basal bodies have radial asymmetry (Beisson and Jerka-Dziadosz, 1999; Iftode and Fleury-Aubusson, 2003). Inside cilia, katanin severed doublet microtubules, whereas the central pair microtubules were unaffected. Within the doublets, the B-tubule was more prone to severing compared with the A-tubule.

Two mechanisms could restrict katanin activity: (1) differential binding of microtubule-associated proteins (MAPs) that sterically block katanin, or (2) differential marking of microtubules with PTMs. It is already known that Tau MAP protects axonal microtubules against katanin severing (Qiang et al., 2006). However, binding of MAPs to microtubules is strongly affected by microtubule PTMs (Bonnet et al., 2001; Peris et al., 2006; Reed et al., 2006). Thus, katanin could be directly or indirectly regulated by PTMs of microtubules.

Katanin and microtubule PTMs could regulate each other

Previously, we described the consequences of mutations that affect the sites of polymodifications on the tail domains of β-tubulin (Thazhath et al., 2002, 2004). We now show that nearly all these defects are also present in the katanin-null mutants. A simple explanation is that katanin requires polymodified microtubules for its transport to proper sites of activity. Recently, acetylation of α-tubulin at Lys-40 was implicated in transport mediated by kinesin-1 (Reed et al., 2006). Alternatively, polymodifications could mark preferred sites for katanin-mediated severing. Importantly, polymodifications occur on the C-terminal tail domains of tubulins and both katanin and spastin require tubulin tails for severing activity (McNally and Vale, 1993; Roll-Mecak and Vale, 2005; White et al., 2007). Furthermore, in *C. elegans*, a substitution of a potentially polymodifiable glutamic acid in the tail domain of β-tubulin rescued lethality associated with overproduction of katanin (Lu et al., 2004), supporting an idea that a polymodified tail of β-tubulin increases katanin activity. Importantly, the known pattern of glutamylation in vivo correlates with the preferred sites of katanin activity revealed by our study. For example, the axonemal B-tubules have higher levels of glutamylation, as compared with the A-tubules and the central pair (Fouquet et al., 1996; Multigner et al., 1996; Lechtreck and Geimer, 2000). The transitional zone appears to lack glutamylation (Lechtreck and Geimer, 2000; Kann et al., 2003) and showed resistance to katanin severing in our study. Furthermore, microtubule types that become hypertrophic in the absence of zygotic katanin in *Tetrahymena* (internal and LMs) are at least monoglutamylated in wild-type cells. The recent identification of tubulin glutamylases (Janke et al., 2005) should allow for a direct test of the role of tubulin glutamylation in katanin activity.

Importantly, we show here that katanin is a negative regulator of PTMs, including polymodifications and acetylation. Katanin could regulate PTM levels directly by recognizing and severing polymodified segments of microtubules. Alternatively, katanin could regulate PTMs indirectly, by increasing the polymer turnover and reducing the time of exposure to modifying enzymes. Thus, katanin and PTMs could regulate each other. Although polymodifications could regulate katanin, it is clear that the resulting severing activity regulates the levels of PTMs on microtubules.

Katanin plays a role in cilia biogenesis

A recent study showed that a mutation of katanin p80 subunit inhibits the central pair formation in *Chlamydomonas* (Dymek et al., 2004). We now show that both subunits of katanin are required for assembly of motile normal-length cilia in *Tetrahymena,* and that lack of the catalytic katanin subunit blocks assembly of the central pair. Collectively, the results of Dymek et al. (2004) and our observations uncover an evolutionarily conserved role of katanin in cilia biogenesis, and in particular its critical role in the central pair assembly. We show that Kat1p p60 has a strong microtubule-severing activity in vivo. It is therefore reasonable to propose that microtubule severing is required for assembly of cilia. Two (non-mutually exclusive) models can be proposed. First, the role of katanin in cilia biogenesis could be indirect and based on the dependence of cilia assembly on proper dynamics of microtubules in extra-ciliary locations. Furthermore, katanin-mediated severing could generate a pool of tubulin dimers or oligomers in the cell body, which could then be used as precursors for ciliary assembly. Although Kat1p-deficient cell chains have normal levels of soluble tubulin and regenerate 9+0 cilia after deciliation, katanin may generate a subpool of precursor tubulin required for the central pair formation. Alternatively, katanin could function inside cilia. Ciliary protein precursors are delivered by the intraflagellar transport (IFT) pathway (Scholey, 2003). It is possible that precursor tubulin transported to ciliary tips by IFT has a form of oligomers or very short microtubules, as has been proposed for tubulin transported inside neural extensions (Terada et al., 2000; Baas et al., 2005). Katanin may be needed inside cilia for fragmentation of an oligomeric tubulin cargo before its assembly. It is intriguing, however, that overexpressed GFP-Kat1p preferentially bound and severed the outer doublets. This activity appears unrelated to deciliation response, as severing occurred outside of the transition zone, and cells lacking zygotic Kat1p p60 underwent deciliation. The association of katanin with doublets could be dismissed as an artifact of an abnormally high level of GFP-Kat1p and the potential high affinity of katanin for polymodified tubulin. In *Chlamydomonas*, however, antibodies detected p80 specifically in the outer doublet compartment (Dymek et al., 2004). Thus, the ciliary function of katanin could

require its association with the outer doublets, possibly based on a novel form of severing of these microtubules that could provide supply of tubulin required for the central pair assembly. Interestingly, we recently found that several Nima A kinases (NRKs) promote depolymerization of axonemal microtubules when overproduced, but accumulate in assembling cilia when expressed at a normal level (Wloga et al., 2006). Thus, a form of turnover of axonemal microtubules mediated by katanin could play a role in the assembly of cilia.

Materials and methods

Bioinformatics

Sequences of AAA domain proteins were obtained from National Center for Biotechnology Information (NCBI) databases. Gene accession numbers of sequences used for phylogenetic analyses are listed in the legend of Fig. S1 (available at http://www.jcb.org/cgi/content/full/jcb.200704021/DC1). The AAA domain sequences were aligned using ClustalX 1.82 and corrected manually in SEAVIEW (Galtier et al., 1996). A tree was calculated using the Phylip package (Felsenstein, 1997). 1,000 replicates of the sequence set were created using SEQBOOT. The distances were calculated in PROTDIST, and trees were reconstructed using NEIGHBOR. The Jones-Taylor-Thorton (JTT) substitution model was used. A consensus tree was obtained using CONSENSE and the tree was plotted using DRAWGRAM.

Germline knockouts

The plasmid constructs were made based on the macronuclear genome sequence of *Tetrahymena thermophila* (Eisen et al., 2006), available at the *Tetrahymena* Genome Database. To prepare a targeting fragment for disruption of *KAT1*, a 4.3-kb macronuclear genomic DNA fragment of *KAT1* was amplified with addition of SacI and ApaI sites and cloned into pBluescript (SK+). The primers used were: 5′-TTATAGAGCTCCTATGTATTTTGAGCAGGTC-3′ and 5′-TATAAGGGCCCGGCTTTTAATGTTCTCTTGA-3′. The pMNBL plasmid (Shang et al., 2002) carrying the *neo3* gene was modified to reduce the size of the *MTT1* promoter to 0.9 kb. The shortened *neo3* cassette of pMNBL starting at the AccI in *MTT1* promoter was subcloned, giving pTvec-neo3. pTvec-neo3 was digested with SpeI to release *neo3*. The cloned *KAT1* genomic fragment was digested with SpeI and *neo3* was inserted, resulting in pTvec-neo3R-KAT1. To prepare a plasmid for disruption of *KAT2*, 1.4 kb of 5′ UTR was amplified with addition of SacI and BamHI sites (primers: 5′-AATTTGAGCTCTGCAAAGCTACTACCAAGAT-3′ and 5′-ATATTGGATCCTTCATACGAGATTCACCTTC-3′) and cloned into p4T2ΔHindIII, a *neo2* cassette plasmid, using SacI and BamHI sites. The resulting plasmid was digested with XhoI and ApaI and used to insert a 1.8-kb fragment of 3′ UTR of *KAT2* (primers: 5′-AATAACTCGAGGTAGACCAAAATAACACACT-3′ and 5′-TATATGGGCCCCCTTTGTTTCTTTGGATTTG -3′), to create pNeo2R-KAT2. To disrupt *KAT3*, a 1.3-kb fragment of 5′ UTR was amplified with addition of SmaI and ApaI restriction sites (primers: 5′-ATAATGGGCCCTACTTAAAATCTTCTTCTTCTA-3′, 5′-AATATCCCGGGTGTTTCTATTTAATGGTTTGTC-3′) and cloned into pTvec-neo3. The resulting plasmid was digested with ClaI and SacI and used to insert an amplified 1.5 kb of the 3′ UTR of *KAT3* (primers 5′-TAATAATCGATGTTTAACGTTGATGGAGAT-3′ and 5′-AATAAGAGCTCGCATCCATAACATAACAAGG -3′) to create pKAT3-neo3R. To disrupt *SPA1*, its 5′ UTR was amplified with addition of SmaI and ApaI sites (primers 5′-TATATGGGCCCAAAGTAGTAAACAAACCTCAAT-3′ and 5′-AATTACCCGGGATTACTTTTTACACTATTCAGC-3′), and cloned into pTvec-neo3. The resulting plasmid was digested with ClaI and SacI and used to clone a 3′ UTR of *SPA1* flanked with ClaI and SacI (primers 5′-TATATATCGATCCATAAGAAATAGACTCAGC-3′ and 5′-ATAAA*GAGCTC*CTAAATAATTGATGTGAACTGA-3′).

For germline targeting, each disruption plasmid was digested with SacI and ApaI and used to transform mating CU428.1 and B2086 strains by biolistic bombardment. Heterokaryons were generated by bringing the micronucleus to homozygosity using a star cross while allowing the disrupted alleles to assort from the macronucleus (Cassidy-Hanley et al., 1997).

Expression of GFP-tagged proteins

To overexpress Kat1p at a high copy number, the coding region of *KAT1* was amplified with primers carrying MluI (5′-TATATACGCGTCATGTCAAATTCAGATAAACAATTA-3′) and BamHI (5′-TAATTGGATCCCTATCAAACAGAACCAAATTCT-3′) sites and cloned into pMTT1-GFP to create pMTT1-GFP-KAT1. To overexpress GFP-Kat2p, the coding region of *KAT2* was amplified with primers carrying MluI (5′-ATTATACGCGTCATGAGTTATCTACTATCAAAA-3′) and BamHI (5′-TAATTGGATCCTCAAACTGAACCATGTTCCTT-3′) restriction sites and cloned into pMTT1-GFP to create pMTT1-GFP-KAT2. To overexpress GFP-Spa1p, the coding region of *SPA1* was amplified with primers carrying MluI (5′-TATATACGCGTCATGGATAGTATC AAAAAAAAAGAAG-3′) and BamHI (5′-TAATTGGATCCTCAAACCTATTT ATTATA CTCTTTG-3′) restriction sites and cloned into pMTT1-GFP to create pMTT1-GFP-SPA1.

To introduce transgenes, starved CU522 cells (from Donna Cassidy-Hanley, Cornell University, Ithaca, NY) were bombarded with a SacI- and XhoI-digested overexpression plasmid, and transformants were selected on SPP medium with 20 μM paclitaxel. Using this approach, the transgene integrates by homologous recombination into the nonessential *BTU1* gene that carries a mutation conferring sensitivity to paclitaxel. The copy number of the transgene was increased by allowing cells to assort the mutant *BTU1* allele during vegetative propagation in the presence of paclitaxel.

To express GFP-Kat1p as a sole Kat1p at a low copy number, we rescued mating *KAT1* heterokaryon progeny from death, by introducing a *KAT1* transgene but without applying any selection directly to increase the transgene copy number. The *KAT1* knockout heterokaryon strains were allowed to complete conjugation during 24 h, transformed biolistically with a BTU1-MTT1-GFP-KAT1-BTU1 fragment. Transformants that integrated the transgene into the *BTU1* locus were selected with paromomycin (120 μg/ml) and cadmium chloride (2.5 μg/ml) (based on cadmium-dependent resistance to paromomycin conferred by the *neo3* gene inserted into the native *KAT1* locus).

Microscopy

We used the immunofluorescence protocol described in Thazhath et al. (2002) for analysis of Kat1p-null cell chains. The immunofluorescence localization of GFP-Kat1p in rescue cells was done as described in Wloga et al. (2006). The following primary antibodies were used: 12G10 anti–α-tubulin (1:10 dilution; mouse monoclonal; University of Iowa, Developmental Studies Hybridoma Bank), 20H5 anti-centrin (1:100; mouse monoclonal; a gift of J. Salisbury, Mayo Clinic, Rochester, MN), anti-total *Tetrahymena* tubulins SG (1:600; rabbit polyclonal; a gift of M. Gorovsky, University of Rochester, Rochester, NY), AXO49 anti-polyglycylated tubulin (1:100; mouse monoclonal (a gift of M.-H. Bré and N. Levilliers, Université Paris-Sud, Orsay, France; Levilliers et al., 1995), ID5 anti-polyglutamylated tubulin (1:10; mouse monoclonal) (a gift of K. Weber, Max Planck Institute, Goettingen, Germany; Rudiger et al., 1999), anti-GFP (1:500; rabbit polyclonal) (Abcam), and 6-11B1 anti-acetylated α-tubulin (1:20; mouse monoclonal) (Sigma-Aldrich). FITC- or Cy-3– conjugated secondary antibodies (Zymed Laboratories) were used at 1:100. Nuclei were stained with DAPI (Sigma-Aldrich). Cells were viewed with a Leica TCS SP2 spectral confocal microscope (using 63× water immersion with 1.2 NA). Images were assembled in Adobe Photoshop 8.0.

For quantitative immunofluorescence, we manually picked mutant cell chains, mixed them with normal cells and processed for immunofluorescence. We used ImageJ to determine the pixel intensity value for areas of cell bodies in mutant and wild-type cells positioned side-by-side on the same confocal section images. 100 randomly selected rectangular areas of 30 × 30 pixels were used to obtain an average pixel intensity, for a total of 10 mutant and 10 adjacent wild-type cells. The average background value was also determined and subtracted from the corresponding intensity values obtained for cell bodies.

For transmission electron microscopy of *KAT1* knockouts, ∼5,000 mutant cell chains were isolated and washed two times with 10 mM Tris HCl buffer at pH 7.5. The cells were fixed in 2% glutaraldehyde in 0.1M sodium cacodylate buffer at pH 7.2 for 1 h at 4°C. Fresh tannic acid was added to 0.01% for 1 h at 4°C. Cells were washed five times with 10 mM Tris pH 7.5 and postfixed in 1% OsO_4 for 1 h at 4°C, washed five times in 4°C with water before dehydration through a graded ethanol series. Cells were transitioned to Epon 812 resin with acetone at 33, 66, and 100% intervals. Cells were infiltrated with 100% Epon for 8 h at 25°C. Fresh 100% Epon was added and allowed to polymerize at 60°C. Ultrathin sections of 50–60 nm were collected and post-stained with uranyl acetate and lead citrate. Sections were visualized on JEOL 100CXII, JOEL 1200 EX, or FEI Technai 20 transmission electron microscopes.

Immunogold labeling was performed on cells expressing GFP-Kat1p at a low copy number as a result of rescue of mating *KAT1* knockout heterokaryons. A post-embedding procedure was performed as described previously (Ueno et al., 2003). Ultrathin sections were immunolabeled with the polyclonal anti-GFP antibody (1:500; Abcam), followed by 10-nm

colloidal gold-conjugated goat anti–rabbit IgG (GE Healthcare). Immunolabeled sections were stained with 2% aqueous uranyl acetate for 30 min and washed several times with distilled water until no signal was detectable in the control sections made for cells not expressing GFP.

Phenotypic tests

To evaluate lethal phenotypes, pairs of mutant heterokaryon strains were allowed to mate and single pairs were isolated into drops of SPP medium 8 h later. The average number of cells and subcells (cortical domains of cell chains) per drop was determined for 48–96 drops at various time intervals using a dissecting scope. To measure the multiplication rate of vegetatively growing strains, cells were diluted to 10^4 cells/ml from a feeder culture of 2×10^5 cells/ml and grown without shaking in 10 ml of SPP. The cell densities were measured every 2 h. In some experiments, to induce MTT1-driven GFP-Kat1p expression, $CdCl_2$ was added at 2.5 μg/ml.

The number of cilia was determined in cells that overproduced GFP-Kat1p. Wild-type cells and uninduced cells were used as controls. Cells were labeled with the anti-tubulin SG antibody (1:500). Cilia number was determined using single confocal section that traversed the widest diameter of the macronucleus. For each time point, 10 different cells were analyzed.

To test the effects of oryzalin and paclitaxel on multiplication of cells lacking zygotic Kat1p, the *KAT1*-null phenotype was induced *en masse* as follows. *KAT1* knockout heterokaryons were grown vegetatively to a density of 2×10^5 cells/ml. Cells were starved in 10 mM Tris-HCl for 24 h and 5 ml of each of the two heterokaryon strains were allowed to mate in a 50-ml conical flask for 24 h. Cells were spun down and suspended in 10 ml SPP to a final concentration of 10^4 cells/ml. Paromomycin (120 μg/ml) and cadmium chloride (2.5 μg/ml) were added to inhibit the growth of nonmating cells (note that between 5–10% of heterokaryon cells do not mate, and therefore retain a wild-type phenotype; these cells were prevented from overgrowing the population by addition of paromomycin based on drug resistance conferred by the selectable markers used for gene disruption). The resulting suspension, highly enriched in exconjugant cells lacking zygotic Kat1p, was incubated in SPP with or without 10 μM paclitaxel, 2 μM oryzalin, or 1% DMSO as a control for 80 h. 10 μl of cell suspension was scored in the DIC microscope and the total number of cells was determined (we scored cell chains as 1 cell regardless of the number of subcells) at 24, 36, 50, 65, and 80 h.

Online supplemental material

Fig. S1 contains a multiple sequence alignment corresponding to the phylogeny of AAA proteins shown in Fig. 2. Fig. S2 shows a lack of a correlation between an arrest in cytokinesis and increased acetylation of microtubules in the cell body (A and B), and documents increased polyglutamylation on cortical microtubules in cells lacking Kat1p (C and D). Fig. S3 documents that cells lacking either Kat2p or Spa1p do not accumulate PTMs on internal microtubules. Fig. S4 documents lack of an effect of overexpression of Kat2p and Spa1p on microtubules and cell multiplication. Fig. S5 shows that cells lacking katanin p60 subunits (Kat1p and Kat2p) undergo deciliation and cilia regeneration. Online supplemental material is available at http://www.jcb.org/cgi/content/full/jcb.200704021/DC1.

We are grateful to Joseph Frankel (University of Iowa) and Edward Kipreos (University of Georgia) for discussing the paper. We thank the following researchers for providing essential reagents: Marie-Helene Bré and Nicolette Levilliers; Martin Gorovsky; Klaus Weber; Jeffrey Salisbury; and Joseph Frankel. The 12G10 antibodies are available from the Developmental Studies Hybridoma Bank developed under the auspices of the National Institute of Child Health and Human Development and maintained by the University of Iowa.

This work was supported by the National Science Foundation award MBC-0235826 (to J. Gaertig), and the statute grant to the Nencki Institute from Committee of Scientific Research (KBN, Poland) (to M. Jerka-Dziadosz). We thank the staff of the Center for Advanced Ultrastructural Studies at University of Georgia and Laboratory for Electron Microscopy at the Nencki Institute for assistance.

Submitted: 4 April 2007
Accepted: 10 August 2007

References

Allen, R.D. 1969. The morphogenesis of basal bodies and accessory structures of the cortex of the ciliate protozoan *Tetrahymena pyriformis*. *J. Cell Biol.* 40:716–733.

Baas, P.W., A. Karabay, and L. Qiang. 2005. Microtubules cut and run. *Trends Cell Biol.* 15:518–524.

Beisson, J., and M. Jerka-Dziadosz. 1999. Polarities of the centriolar structure: morphogenetic consequences. *Biol. Cell.* 91:367–378.

Bichet, A., T. Desnos, S. Turner, O. Grandjean, and H. Hofte. 2001. BOTERO1 is required for normal orientation of cortical microtubules and anisotropic cell expansion in Arabidopsis. *Plant J.* 25:137–148.

Bonnet, C., D. Boucher, S. Lazereg, B. Pedrotti, K. Islam, P. Denoulet, and J.C. Larcher. 2001. Differential binding regulation of microtubule-associated proteins MAP1A, MAP1B, and MAP2 by tubulin polyglutamylation. *J. Biol. Chem.* 276:12839–12848.

Burk, D.H., B. Liu, R. Zhong, W.H. Morrison, and Z.H. Ye. 2001. A katanin-like protein regulates normal cell wall biosynthesis and cell elongation. *Plant Cell.* 13:807–827.

Cassidy-Hanley, D., J. Bowen, J.H. Lee, E. Cole, L.A. VerPlank, J. Gaertig, M.A. Gorovsky, and P.J. Bruns. 1997. Germline and somatic transformation of mating *Tetrahymena thermophila* by particle bombardment. *Genetics*. 146:135–147.

Dymek, E.E., P.A. Lefebvre, and E.F. Smith. 2004. PF15p is the *Chlamydomonas* homologue of the Katanin p80 subunit and is required for assembly of flagellar central microtubules. *Eukaryot. Cell.* 3:870–879.

Eddé, B., J. Rossier, J.-P. Le Caer, E. Desbruyeres, F. Gros, and P. Denoulet. 1990. Posttranslational glutamylation of α-tubulin. *Science.* 247:83–85.

Eisen, J.A., R.S. Coyne, M. Wu, D. Wu, M. Thiagarajan, J.R. Wortman, J.H. Badger, Q. Ren, P. Amedeo, K.M. Jones, et al. 2006. Macronuclear genome sequence of the ciliate *Tetrahymena thermophila*, a model eukaryote. *PLoS Biol.* 4:e286.

Felsenstein, J. 1997. An alternating least squares approach to inferring phylogenies from pairwise distances. *Syst. Biol.* 46:101–111.

Fouquet, J.P., Y. Prigent, and M.L. Kann. 1996. Comparative immunogold analysis of tubulin isoforms in the mouse sperm flagellum: unique distribution of glutamylated tubulin. *Mol. Reprod. Dev.* 43:358–365.

Frankel, J., E.M. Nelsen, and L.M. Jenkins. 1981. Development of the ciliature of *Tetrahymena thermophila*. II. Spatial subdivision prior to cytokinesis. *Dev. Biol.* 88:39–54.

Gaertig, J., M.A. Cruz, J. Bowen, L. Gu, D.G. Pennock, and M.A. Gorovsky. 1995. Acetylation of lysine 40 in alpha-tubulin is not essential in *Tetrahymena thermophila*. *J. Cell Biol.* 129:1301–1310.

Galtier, N., M. Gouy, and C. Gautier. 1996. SEAVIEW and PHYLO_WIN: two graphic tools for sequence alignment and molecular phylogeny. *Comput. Appl. Biosci.* 12:543–548.

Hartman, J.J., and R.D. Vale. 1999. Microtubule disassembly by ATP-dependent oligomerization of the AAA enzyme katanin. *Science.* 286:782–785.

Hazan, J., N. Fonknechten, D. Mavel, C. Paternotte, D. Samson, F. Artiguenave, C.S. Davoine, C. Cruaud, A. Durr, P. Wincker, et al. 1999. Spastin, a new AAA protein, is altered in the most frequent form of autosomal dominant spastic paraplegia. *Nat. Genet.* 23:296–303.

Iftode, F., and A. Fleury-Aubusson. 2003. Structural inheritance in *Paramecium*: ultrastructural evidence for basal body and associated rootlets polarity transmission through binary fission. *Biol. Cell.* 95:39–51.

Janke, C., K. Rogowski, D. Wloga, C. Regnard, A.V. Kajava, J.-M. Strub, N. Temurak, J. van Dijk, D. Boucher, A. van Dorsselaer, et al. 2005. Tubulin polyglutamylase enzymes are members of the TTL domain protein family. *Science.* 308:1758–1762.

Kann, M.L., S. Soues, N. Levilliers, and J.P. Fouquet. 2003. Glutamylated tubulin: diversity of expression and distribution of isoforms. *Cell Motil. Cytoskeleton.* 55:14–25.

Lechtreck, K.-F., and S. Geimer. 2000. Distributon of polyglutamylated tubulin in the flagellar apparatus of green flagellates. *Cell Motil. Cytoskeleton.* 47:219–235.

Levilliers, N., A. Fleury, and A.M. Hill. 1995. Monoclonal and polyclonal antibodies detect a new type of post-translational modification of axonemal tubulin. *J. Cell Sci.* 108:3013–3028.

Lohret, T.A., F.J. McNally, and L. Quarmby. 1998. A role for katanin-mediated axonemal severing during *Chlamydomonas* defalgellation. *Mol. Biol. Cell.* 9:1195–1207.

Lu, C., M. Srayko, and P.E. Mains. 2004. The *Caenorhabditis elegans* microtubule-severing complex MEI-1/MEI-2 katanin interacts differently with two superficially redundant beta-tubulin isotypes. *Mol. Biol. Cell.* 15:142–150.

McNally, F.J., and R.D. Vale. 1993. Identification of katanin, an ATPase that severs and disassembles stable microtubules. *Cell.* 75:419–429.

McNally, F.J., and S. Thomas. 1998. Katanin is responsible for the M-phase microtubule-severing activity in *Xenopus* eggs. *Mol. Biol. Cell.* 9:1847–1861.

McNally, K., A. Audhya, K. Oegema, and F.J. McNally. 2006. Katanin controls mitotic and meiotic spindle length. *J. Cell Biol.* 175:881–891.

Multigner, L., I. Pignot-Paintrand, Y. Saoudi, D. Job, U. Plessmann, M. Rüdiger, and K. Weber. 1996. The A and B tubules of the outer doublets of sea urchin sperm axonemes are composed of different tubulin variants. *Biochemistry.* 35:10862–10871.

Orso, G., A. Martinuzzi, M.G. Rossetto, E. Sartori, M. Feany, and A. Daga. 2005. Disease-related phenotypes in a *Drosophila* model of hereditary spastic paraplegia are ameliorated by treatment with vinblastine. *J. Clin. Invest.* 115:3026–3034.

Peris, L., M. Thery, J. Faure, Y. Saoudi, L. Lafanechere, J.K. Chilton, P. Gordon-Weeks, N. Galjart, M. Bornens, L. Wordeman, et al. 2006. Tubulin tyrosination is a major factor affecting the recruitment of CAP-Gly proteins at microtubule plus ends. *J. Cell Biol.* 174:839–849.

Piperno, G., M. Ledizet, and X.J. Chang. 1987. Microtubules containing acetylated α-tubulin in mammalian cells in culture. *J. Cell Biol.* 104:289–302.

Pitelka, D.R. 1961. Fine structure and silver line and fibrillar systems of three tetrahyminid species. *J. Protozool.* 8:75–89.

Qiang, L., W. Yu, A. Andreadis, M. Luo, and P.W. Baas. 2006. Tau protects microtubules in the axon from severing by katanin. *J. Neurosci.* 26:3120–3129.

Quarmby, L.M. 2004. Cellular deflagellation. *Int. Rev. Cytol.* 233:47–91.

Redeker, V., N. Levilliers, J.-M. Schmitter, J.-P. Le Caer, J. Rossier, A. Adoutte, and M.-H. Bré. 1994. Polyglycylation of tubulin: a post-translational modification in axonemal microtubules. *Science.* 266:1688–1691.

Reed, N.A., D. Cai, L. Blasius, G.T. Jih, E. Meyhofer, J. Gaertig, and K.J. Verhey. 2006. Microtubule acetylation promotes kinesin-1 binding and transport. *Curr. Biol.* 16:2166–2172.

Roll-Mecak, A., and R.D. Vale. 2005. The *Drosophila* homologue of the hereditary spastic paraplegia protein, spastin, severs and disassembles microtubules. *Curr. Biol.* 15:650–655.

Rudiger, A.H., M. Rudiger, J. Wehland, and K. Weber. 1999. Monoclonal antibody ID5: epitope characterization and minimal requirements for the recognition of polyglutamylated alpha- and beta-tubulin. *Eur. J. Cell Biol.* 78:15–20.

Scholey, J.M. 2003. Intraflagellar transport. *Annu. Rev. Cell Dev. Biol.* 19:423–443.

Shang, Y., X. Song, J. Bowen, R. Corstanje, Y. Gao, J. Gaertig, and M.A. Gorovsky. 2002. A robust inducible-repressible promoter greatly facilitates gene knockouts, conditional expression, and overexpression of homologous and heterologous genes in *Tetrahymena thermophila*. *Proc. Natl. Acad. Sci. USA.* 99:3734–3739.

Sherwood, N.T., Q. Sun, M. Xue, B. Zhang, and K. Zinn. 2004. *Drosophila* spastin regulates synaptic microtubule networks and is required for normal motor function. *PLoS Biol.* 2:e429.

Srayko, M., D.W. Buster, O.A. Bazirgan, F.J. McNally, and P.E. Mains. 2000. MEI-1/MEI-2 katanin-like microtubule severing activity is required for *Caenorhabditis elegans* meiosis. *Genes Dev.* 14:1072–1084.

Srayko, M., E.T. O'toole E, A.A. Hyman, and T. Müller-Reichert. 2006. Katanin disrupts the microtubule lattice and increases polymer number in *C. elegans* meiosis. *Curr Biol.* 16:1944–1949.

Stargell, L.A., D.P. Heruth, J. Gaertig, and M.A. Gorovsky. 1992. Drugs affecting microtubule dynamics increase α-tubulin mRNA accumulation via transcription in *Tetrahymena thermophila. Mol. Cell. Biol.* 12:1443–1450.

Tarrade, A., C. Fassier, S. Courageot, D. Charvin, J. Vitte, L. Peris, A. Thorel, E. Mouisel, N. Fonknechten, N. Roblot, et al. 2006. A mutation of spastin is responsible for swellings and impairment of transport in a region of axon characterized by changes in microtubule composition. *Hum. Mol. Genet.* 15:3544–3558.

Terada, S., M. Kinjo, and N. Hirokawa. 2000. Oligomeric tubulin in large transporting complex is transported via kinesin in squid giant axons. *Cell.* 103:141–155.

Thazhath, R., C. Liu, and J. Gaertig. 2002. Polyglycylation domain of beta-tubulin maintains axonemal architecture and affects cytokinesis in *Tetrahymena*. *Nat. Cell Biol.* 4:256–259.

Thazhath, R., M. Jerka-Dziadosz, J. Duan, D. Wloga, M.A. Gorovsky, J. Frankel, and J. Gaertig. 2004. Cell context-specific effects of the beta-tubulin glycylation domain on assembly and size of microtubular organelles. *Mol. Biol. Cell.* 15:4136–4147.

Trotta, N., G. Orso, M.G. Rossetto, A. Daga, and K. Broadie. 2004. The hereditary spastic paraplegia gene, spastin, regulates microtubule stability to modulate synaptic structure and function. *Curr. Biol.* 14:1135–1147.

Ueno, H., K. Gonda, T. Takeda, and O. Numata. 2003. Identification of elongation factor-1alpha as a Ca2+/calmodulin-binding protein in *Tetrahymena* cilia. *Cell Motil. Cytoskeleton.* 55:51–60.

White, S.R., K.J. Evans, J. Lary, J.L. Cole, and B. Lauring. 2007. Recognition of C-terminal amino acids in tubulin by pore loops in Spastin is important for microtubule severing. *J. Cell Biol.* 176:995–1005.

Wloga, D., A. Camba, K. Rogowski, G. Manning, M. Jerka-Dziadosz, and J. Gaertig. 2006. Members of the Nima-related kinase family promote disassembly of cilia by multiple mechanisms. *Mol. Biol. Cell.* 17:2799–2810.

Xia, L., B. Hai, Y. Gao, D. Burnette, R. Thazhath, J. Duan, M.-H. Bré, N. Levilliers, M.A. Gorovsky, and J. Gaertig. 2000. Polyglycylation of tubulin is essential and affects cell motility and division in *Tetrahymena thermophila. J. Cell Biol.* 149:1097–1106.

Zhang, D., G.C. Rogers, D.W. Buster, and D.J. Sharp. 2007. Three microtubule severing enzymes contribute to the "Pacman-flux" machinery that moves chromosomes. *J. Cell Biol.* 177:231–242.